4644 *Macromolecules* **2007,** *40,* 4644−4653

Effect of Adsorption History on the Surface Morphology of a Self-Associating Diblock Copolymer: A Surface Forces Study

Scott C. McLean and Michelle L. Gee*

School of Chemistry, The University of Melbourne, Parkville, Victoria 3010, Australia

Received March 20, 2007

ABSTRACT: We have investigated the history-dependent adsorption behavior of the diblock copolymer P2VP−PEO. The solution self-assembly of this polymer is pH-tunable such that micelles with a P2VP core and a PEO corona are formed above the polymer's pK_a of 5.9. In-situ attenuated total reflection and atomic force microscopy were used to measure the polymer surface excess and obtain direct force measurements between the silica-adsorbed P2VP−PEO layers, respectively. It was found that well above the pK_a of P2VP−PEO where it micellizes the polymer adsorbs to silica and remains self-assembled. However, at pH 3.6 when initial adsorption of the polymer is as a unimer, an increase in solution pH to above the polymer's pK_a does not result in surface self-assembly since the cooperative detachment from the surface of a large number of polymer segments required to achieve this is energetically costly. A decrease in solution pH to below its pK_a brings about micelle disassembly with no polymer desorption. This is driven by the increased electrostatic segment−segment repulsion between the now ionized P2VP segments and the increase in affinity the polymer has for the negatively charged silica surface through attractive electrostatic interactions between silica and the ionized P2VP segments. At solution pH's near and below its pK_a, P2VP−PEO exhibits ergodic behavior. A pH change from 3.6 to 6.6 or visa versa results in a subtle difference in surface morphology that can be explained in terms of changes in the electrostatic attraction between the P2VP block and the surface. This change in surface morphology between these two pH's appears reversible.

Introduction

Amphiphilic diblock copolymers are known to self-assemble in water to form micellar structures, with a hydrophobic core surrounded by a hydrophilic polymer shell.[1] Such polymeric micelles have potential in bioseparations and the cosmetics industry[2,3] and as pigment stabilizers in water-borne coatings.[4] Recently, there has also been considerable attention shown in the development of these polymeric micelles for use as controlled drug delivery systems.[5,6] In each of these applications, it is the ability of the polymeric micelle to encapsulate and protect a water-insoluble material within its hydrophobic core that is exploited. The advantage of polymeric micelles is that they are structurally robust in contrast to surfactant micelles which are dynamic structures.[7] Hence in drug delivery, for example, a polymeric micelle with a biocompatible exterior is able to transport a drug throughout the circulatory system without breaking down while minimizing the removal of the drug from the body.[8] Of particular interest in controlling the delivery of anticancer drugs are the "double hydrophilic" diblock copolymer systems.[9,10] These diblock copolymers contain two water-soluble blocks. The solubility of one of the blocks is pH-tunable[11] and, consequently, so too is polymer self-assembly. For example, the pH-sensitive diblock copolymer poly(2-vinylpyridine)−poly(ethylene oxide) (P2VP−PEO)[12,13] self-assembles in water to form micelles when the pH is above the pK_a of the P2VP block (pK_a ∼5.9). At pH's below the pK_a of P2VP, the diblock exists as a unimer in solution. In the work of Gohy et al.,[13,14] the self-assembly of this diblock copolymer in aqueous solution was investigated using a combination of static light scattering, dynamic light scattering, and transmission electron microscopy. These investigations yielded information on the shape (spherical), hydrodynamic radius (∼25 nm), and inferred aggregation number (∼250) of this diblock micelle in water. Additionally, the radius of gyration for the micelle was found to be ∼60 nm.[13] We have recently performed small-angle neutron scattering measurements[15] that indicate a somewhat nonspherical structure and a lower aggregation number (77−87) than previously reported, but an effective micelle radius of 22 nm, comparable to the hydrodynamic radius of the micelle obtained from light-scattering measurements.

In many of the potential applications of pH-tunable polymeric micelles, e.g., as coatings[4] or in targeted drug delivery,[8] it is their adsorption at an interface that is important. The surface morphologies of such self-assembled structures upon adsorption at the solid−liquid interface have been studied extensively.[16−32] However, many of these investigations were performed in air after having dried the adsorbed layer.[16−19] There is a recent emergence of work focusing on the surface morphology of self-assembled polymeric structures adsorbed from aqueous solution to the solid−liquid interface in situ.[20−32] Much of this recent work has been undertaken by Webber et al.,[26−29] using atomic force microscopy (AFM) to image the adsorbed polymeric micelles, in situ. Their initial investigation focused on the micellar adsorption behavior of the diblock copolymer poly(2-(dimethylamino)ethyl methacrylate)−poly(methyl methacrylate) (PDMA−PMMA).[26] This diblock adsorbs at low pH as individual micelles that are arranged over the surface in a disordered manner. These micelles, however, are not pH-tunable. With an increase in pH, the PDMA−PMMA micelles adopt a close-packed surface structure.[26] In subsequent work[27−29] the diblock copolymer poly(2-(dimethylamino)ethyl methacrylate)−poly-(2-(diethylamino)ethyl methacrylate) (PDMA−PDEA) was studied. This diblock, however, does self-assemble in water depending on solution pH. The surface morphology of these adsorbed polymeric micelles was found to be dependent on both solution pH and the degree of quaternarization of the PDMA block.[27−29] For example, a lowering of the solution pH was observed to bring about a change in surface morphology, from

---

* To whom correspondence should be addressed.

10.1021/ma0706780 CCC: $37.00

adsorbed micelles to localized polymer brushes. The original morphology was regained once the pH was cycled back to a high pH.[28] The lightly quarternized micelles, however, were found to swell irreversibly upon lowering solution pH,[27] while a complete loss of surface morphology was observed with the highly quarternized micelles.[29]

As noted above, the behavior of the pH-sensitive diblock copolymer poly(2-vinylpyridine)−poly(ethylene oxide) (P2VP−PEO) in solution has been investigated.[13−15] In the present work, however, we are interested in studying the adsorption characteristics of this diblock copolymer (P2VP−PEO). What sets this diblock apart from others that have been investigated[27−29] is its biocompatibility when in the micellar state since its exterior is the highly biocompatible PEO block.[7,33,34] Such biocompatible systems are of particular importance in biological applications like targeted drug delivery. Hence, we have investigated the adsorption behavior of P2VP−PEO on silica as a function of solution pH, in situ, by direct force measurements using AFM. The history dependence of this system was also investigated, since many polymeric systems are nonergodic.[35−37] Note we did not image the adsorbed polymer using AFM as in previous work since imaging on a neutrally charged, highly deformable layer does not facilitate detailed morphological information.[22] To complement these surface forces data, the P2VP−PEO surface excess has been obtained using UV−vis attenuated total reflection (ATR) spectroscopy.

Experimental Section

Materials. The silica spheres used in the atomic force microscopy (AFM) measurements were a gift from Allied Signal (Des Plaines, IL). They were prepared by a modified Stöber process[38] and have a diameter between 4 and 6 μm, as measured by high-magnification optical microscopy. The flat silica (Suprasil) surfaces for force measurement studies were obtained from H.A. Groiss Ltd. (Wantirna, VIC). The AFM cantilevers tips (Digital Instruments, Santa Barbara, CA) had spring constants of either 0.11 or 0.292 N m^{-1}, as measured below. The glue used to attach the silica particles to the AFM cantilevers (EPON 1004) was obtained from Shell.

The silica (Suprasil) waveguides for the attenuated total reflection measurements were supplied by H.A. Groiss Ltd. with dimensions of 50 × 20 × 2 mm. The entrance and exit faces were bevelled to 70°. The reflective faces were polished to a peak-to-trough roughness of less than 2 nm and periodicity of 40 nm.

Water used in both cleaning and solution preparation was purified using a Milli-Q Plus water purification system fed by a reverse osmosis water purification system, yielding water with a resistivity of 18.2 MΩ cm^{-1}.

AR grade potassium nitrate, sodium hydroxide, nitric acid, hydrogen peroxide, ammonia, and ethanol were used as received (Merck, Kilsyth VIC). Acridine (Sigma, St. Louis, MO) was used as received.

The poly(2-vinylpyridine)−poly(ethylene oxide) (P2VP−PEO) was obtained from Polymer Source (Montreal, Canada). The P2VP block has 41 repeat units, and the PEO block has 204 repeat units. The polymer is very monodisperse with a M_w/M_n ratio 1.05, where M_w and M_n are the weight-average and number-average molecular weights, respectively. The chemical structures of P2VP and PEO are shown in Figure 1. Below pH 6 P2VP−PEO exists in solution as a unimer, and above this pH the diblock self-associates to form polymeric micelles and has a critical micelle concentration (cmc) of 150−200 ppm (unpublished data).

Experimental Methodologies. *Surface Forces Measurements.* The interaction forces between two silica surfaces bearing adsorbed polymer were measured using a Multimode atomic force microscope (AFM) with a Nanoscope III controller (Digital Instruments, Inc.) and the colloid probe method developed by Ducker et al.[39] In this method, a silica sphere is attached to the microfabricated cantilever spring used in the AFM, providing a sphere on flat geometry for surface forces measurements. To scale the force measurements correctly, the spring constant must be known accurately. This was achieved using the resonance method proposed by Cleveland et al.,[40] giving a spring constant with an error of ∼10%. An average value calculated from a sample of 10 cantilevers was used to scale the raw data obtained from the direct force measurements. An approach rate of 684 nm/s, corresponding to a scan rate of 0.5 Hz, was used in all force measurements. Since the hydrodynamic force will only contribute minimally to the net force at this approach rate,[41] the force profiles can be considered to be obtained under "quasi-equilibrium" conditions. A minimum of 20 force curves were obtained for each set of solution conditions. Note that consecutive force runs at the same point of contact were found to be reproducible under each set of solution conditions.

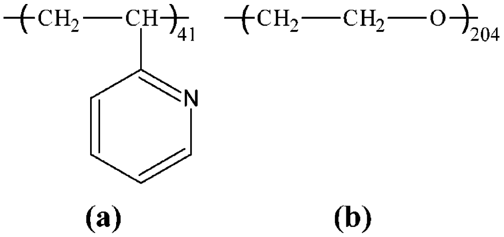

Figure 1. Chemical structure of poly(2-vinylpyridine)−poly(ethylene oxide) (P2VP−PEO): poly(2-vinylpyridine) **(**a**)** and poly(ethylene oxide) **(**b**)**.

Prior to all force measurements involving P2VP−PEO, the bare silica surfaces were characterized by measuring their interaction in a 10^{-3} M KNO_3 solution at natural pH (pH 5.6). A stock solution containing 500 ppm P2VP−PEO was prepared with a background electrolyte concentration of 10^{-3} M KNO_3. 10 mL of the stock P2VP−PEO solution, adjusted to a specific pH, was then injected into the cell and allowed to come to equilibrium with the silica surfaces for 12 h before any surface forces measurements. Since the volume injected is ∼100 times the volume of the cell, complete removal of the previous solution is ensured. Subsequent changes to pH of the system were accomplished by similarly flushing the cell with 10 mL of pH-adjusted stock solution. After each pH adjustment the system was allowed to equilibrate for 12 h prior to any force measurements.

Surface Excess Measurements. Attenuated total reflection (ATR) spectroscopy[42] was used to determine the surface excess of silica-adsorbed P2VP−PEO using a purpose-built single-beam UV−vis ATR spectrophotometer, described elsewhere.[43] Before each experiment, the silica waveguide was calibrated for the number of reflections and hence the effective path length of the evanescent wave, as described previously.[44] The transmission spectrum of the surface-adsorbed diblock copolymer was measured using the intrinsic absorbance of the vinylpyridine group. The number of reflections obtained in the calibration was then used to convert ATR absorbance measurements to P2VP−PEO surface excess.

Prior to each experiment a stock solution was prepared containing 500 ppm P2VP−PEO with a background electrolyte concentration of 1 × 10^{-3} M KNO_3 and adjusted to a specific pH. This stock solution was then pumped from a remote reservoir into the fluid cell housing the silica ATR element. Transmission spectra were then collected every 30 min for 12 h, under quiescent conditions. Changes in system pH were achieved by adjusting the pH of solution in the reservoir. Solution from the reservoir was then circulated through the ATR fluid cell until the pH was stable.

Adsorption Schemes. To study the effect pH has on the adsorption characteristics of P2VP−PEO to silica, both surface excess and surface forces were measured as a function of solution pH, as described above. Any history dependence in the adsorption behavior of the polymer was probed by adopting two adsorption schemes that we have named pH high−low and pH low−high, respectively. Under the pH high−low scheme, P2VP−PEO was initially adsorbed onto bare silica at high solution pH, specifically pH 9.3. Once measurements of the intersurface forces and surface excess were performed, the solution pH was decreased for subsequent measure-

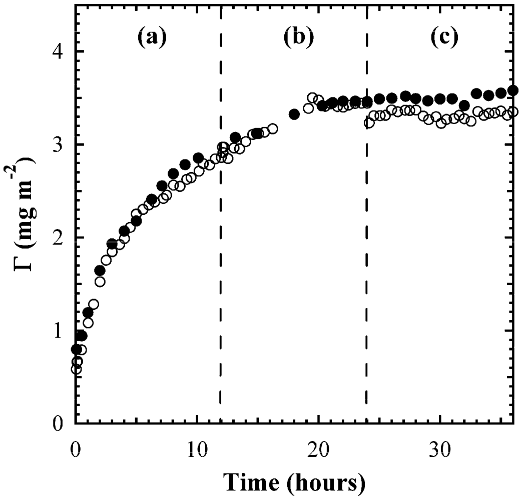

Figure 2. Surface excess as a function of time for the adsorption of P2VP−PEO onto silica from a 500 ppm, 10^{-3} M KNO_3 aqueous solution: (●) the polymer is initially adsorbed at pH 9.3 and the surface excess monitored at this pH for 36 h; (○) the polymer is initially adsorbed at a solution pH of 9.3 (a), followed by a pH decreases to pH 6.6 (b) and then to pH 3.6 (c) at 12 h intervals.

ments. The surface forces profile for the interaction between two silica-adsorbed P2VP−PEO layers and the corresponding polymer surface excess were thus obtained at pH 9.3, 6.6, and 3.6.

Similarly, under the pH low−high scheme, P2VP−PEO was initially adsorbed onto bare silica at low solution pH, i.e., pH 3.6, and sequentially changed to pH 6.6 and then pH 9.3 for surface forces and surface excess measurements.

Cleaning Protocol. Volumetric glassware was soaked overnight in 10% (v/v) nitric acid and rinsed thoroughly with Milli-Q water immediately prior to use. All other glassware was soaked in sodium hydroxide (10% w/w) for 60 min and rinsed with copious amounts of Milli-Q water prior to use.

The AFM fluid cell, tube fittings, O-ring, tweezers, substrates, and syringes were soaked in RBS 35 (Pierce, Rockford, IL) surfactant solution overnight, rinsed with copious amounts of Milli-Q water, and soaked in AR ethanol overnight. Immediately prior to each experiment the equipment was blown dry with nitrogen gas (BOC Gases), filtered through an activated carbon and moisture trap. To ensure that the AFM fluid cell, hydrophilic silica substrates, and cantilevers with attached silica spheres were rendered clean and free of surface impurities, they were ozone scrubbed according to the method of Vig.[45] In this method the components are cleaned by placing them under a UV light in the presence of water vapor before installation into the AFM.

The stainless steel ATR cell, solution vessel, and tweezers were soaked overnight in Extran 100 (Merck, Kilsyth VIC), thoroughly rinsed with Milli-Q water, immersed in concentrated (∼10%) nitric acid overnight, and then rinsed with copious amounts of Milli-Q water. All other fittings were sonicated for 90 min in Extran 100, rinsed with Milli-Q water, soaked in concentrated NaOH, rinsed, and then boiled extensively in Milli-Q water. Immediately prior to the assembly of the cell, the silica waveguide was immersed in a heated solution of 1 vol % concentrated NH_3 in 49% w/v H_2O_2 for about an hour and then rinsed with copious amount of Milli-Q water.[46]

Results and Discussion

Surface Excess Measurements. The adsorption from solution of P2VP−PEO onto silica at pH 9.3 was measured as a function of time. These data are shown in Figure 2. Note that there is an initial rapid increase in the surface excess of P2VP−PEO, as is typical of adsorption rate measurements.[47] The surface excess plateaus after ∼24 h to a value of 3.5 mg m^{-2}. Also shown in Figure 2 are data from a separate experiment in which the surface excess as a function of time was measured for initial adsorption at pH 9.3 followed by a pH decrease to 6.6 and then to 3.6 at 12 h intervals, i.e., the high−low adsorption scheme. These time intervals correspond to sections (a), (b), and (c) in Figure 2, respectively. It is interesting to note the marked similarity between the two curves. Clearly, when P2VP−PEO is initially adsorbed onto silica from solution at high pH, subsequent decreases in pH do not perturb the adsorption kinetics from that obtained at pH 9.3. The implication is that when P2VP−PEO is initially adsorbed at pH 9.3, adsorption is irreversible, in relation to changes in solution pH. This irreversibility is more apparent when comparing these observations to what is seen when the polymer is initially adsorbed at pH 3.6 (Figure 3). Here the surface excess plateaus after ∼10 h at the initial pH of 3.6, implying attainment of equilibrium. This is a far more rapid equilibrium than the 24 h required for equilibrium when initial adsorption is from a pH 9.3 solution. Further highlighting the irreversibility is a comparison of the equilibrium surface excesses at pH 3.6 for the two adsorption schemes. When initially adsorbed at pH 3.6, the surface excess plateaus at around 2.6 mg m^{-2}. When the polymer is adsorbed at pH 9.3, at which the equilibrium surface excess is 3.5 mg m^{-2}, decreasing pH to 3.6 as per the high−low adsorption scheme does not result in any desorption.

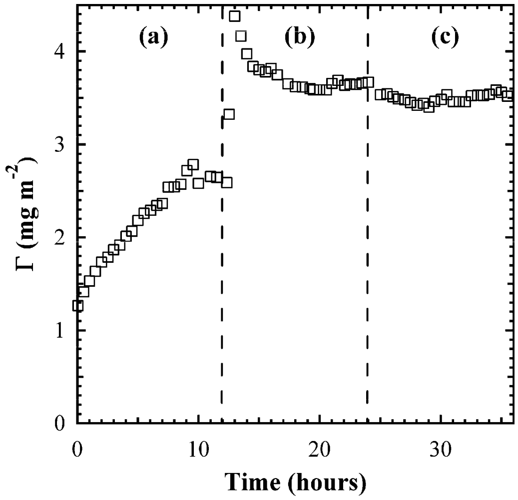

Figure 3. Surface excess as a function of time for the adsorption of P2VP−PEO adsorbed onto silica from a 500 ppm, 10^{-3} M KNO_3 aqueous solution. The polymer is initially adsorbed at pH 3.6 (a) and then pH is subsequently increased to pH 6.6 (b) and then pH 9.3 (c) at 12 h intervals.

Interestingly, after adsorption at pH 3.6 (Figure 3), a subsequent increase in pH to 6.6 after 12 h results in a rapid increase in surface excess to a plateau value corresponding to that obtained for the high−low adsorption scheme (Figure 2). A further increase to pH 9.3 does not appear to perturb equilibrium. Indeed, the equilibrium surface excess of P2VP−PEO at pH 9.3 is independent of the pH of initial adsorption.

These adsorption data are used in the interpretation of the surface forces measurements in the discussion that follows.

Surface Forces Measurements. It should be noted that the absolute zero surface separation in this set of experiments is zero separation between the silica sphere and the silica flat. In an AFM force experiment, zero surface separation is the point at which constant compliance is obtained. If the surfaces bear some adsorbed species, constant compliance occurs when the adsorbed layers are fully compressed.[48] In this region of zero compressibility, there is a linear relationship between the cantilever deflection and the piezo travel. The thickness of these

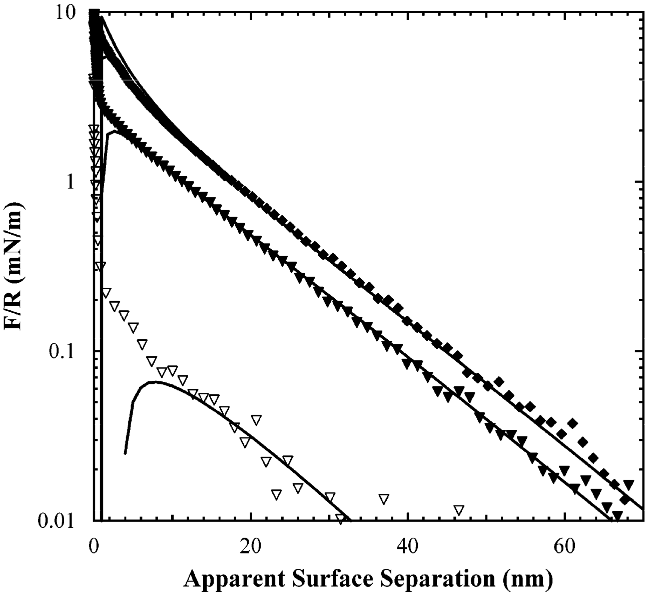

Figure 4. Surface forces profiles for the interaction between a silica sphere and a flat silica surface in a 10^{-3} M KNO_3 aqueous solution as a function of solution pH. The scaled force, *F*/*R*, is plotted as a function of apparent surface separation for solution pH's of (▽) 3.6, (▼) 6.9, and (◆) 9.3. The solid lines are the theoretical DLVO fits to the experimental data calculated using the algorithm of McCormack et al.[35]

fully compressed layers is a somewhat arbitrary value and depends on polymer surface conformation, chain length, etc. In the force vs apparent surface separation data presented here, zero surface separation corresponds to the separation from which the P2VP−PEO layers are incompressible.

Characterization of Silica−Silica Surface Forces. Interaction forces between a silica sphere and a silica flat were measured as a function of surface separation at pH 3.6, 6.9, and 9.3 in a 10^{-3} M KNO_3 aqueous solution, as a benchmark for the surface forces between adsorbed polymer layers described below. The resulting force profiles are shown in Figure 4 and are plotted on a semilog scale to facilitate identification of double-layer interactions forces since they decay exponentially with surface separation. Each force profile was fitted to DLVO theory using a numerical solution to the nonlinear Poisson−Boltzmann equation calculated using the algorithm of McCormack et al.[49] and a Hamaker constant of 0.833×10^{-20} J.[50] These fits appear as the solid lines in Figure 4. The interaction at each pH is purely repulsive, decreasing linearly with surface separation typical of a purely DLVO interaction. Note the Debye length obtained from the slope of each force profile is 10 ± 1 nm, in agreement with that expected for the interaction between two charged interfaces in 10^{-3} M, 1:1 electrolyte.[51] The DLVO fits to the data yield surface potentials of −18, −76, and −115 mV at solution pH's of 3.6, 6.9, and 9.3, respectively. All these data are in good agreement with those previously reported for this system.[51]

Surface Forces between Silica-Adsorbed P2VP−PEO Layers. *Surface Interactions between Silica-Adsorbed P2VP−PEO Initially Adsorbed at pH 9.3, as a Function of pH.* Figure 5 shows the surface forces profile after equilibration of the silica surfaces with a 10^{-3} M KNO_3 solution containing P2VP−PEO at pH 9.3, as per the pH high−low adsorption scheme. This is compared to the bare silica−silica interaction under the same solution conditions, in the absence of polymer. Both force profiles are linearly repulsive on a semilog scale, as is typical of a DLVO type interaction, but clearly the presence of the P2VP−PEO significantly reduces the range of the repulsion.

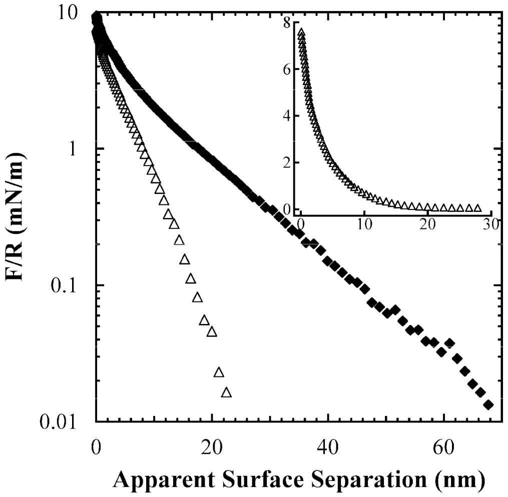

Figure 5. Surface forces profile for the interaction between two silica surfaces at a solution pH of 9.3 in 10^{-3} M KNO_3 (◆) is compared to the surface forces profile for the interaction between two silica-adsorbed P2VP−PEO layers under the same solution conditions (△). In the case of the polymer−polymer interactions, P2VP−PEO was adsorbed from an aqueous solution at pH 9.3 containing 500 ppm P2VP−PEO at 10^{-3} M KNO_3. Measurements were taken after 12 h to ensure equilibrium between adsorbed polymer and free polymer in solution. The inset contains this same surface forces profile on a linear scale.

(The inset in Figure 5 illustrates the reduced range more clearly on a linear−linear plot.) In order to attempt to fit the P2VP−PEO force profile to DLVO theory, it was necessary to assume zero separation to be the onset of the hard-wall repulsion (see above). A Hamaker constant for the interaction between two highly hydrated polymer layers across water was estimated to be 10^{-20} J using the method of Hough and White.[50] Note that this estimate has ignored the effect of the underlying silica substrate since it is negligible at short range from a thick polymer layer is adsorbed to the surface, and its inclusion would only impact slightly on the predicted DLVO interaction at long range. The attempt to fit the P2VP−PEO force profile to DLVO theory yields a Debye length of 4 ± 1 nm. This is significantly less than the 10 nm Debye length obtained for the DLVO type silica−silica interaction. Indeed, from DLVO theory, a Debye length of 4 nm is expected for the interaction of two charged interfaces in a 1:1 electrolyte at much higher concentration (7×10^{-3} M) to that used here. It is unlikely that P2VP−PEO in solution has increased electrolyte concentration since it was supplied in its acidic form and has little or no charge at pH 9.3. The net repulsive force profile for the interaction of two adsorbed P2VP−PEO layers cannot therefore be attributed to a DLVO type interaction and hence is most likely steric or electrosteric in origin. Such intersurface repulsive forces in polymer systems have a contribution from the entropic confinement of the polymer chains, and if the polymer contains some charged groups, an additional electrostatic repulsion between approaching similarly charged polyelectrolyte segments.[52,53] There is also a possible electrostatic contribution from the underlying silica surface.

On first inspection, a subsequent decrease in solution pH from 9.3 to 6.6 appears to have minimal impact on the interaction between the two silica-adsorbed P2VP−PEO layers. This is illustrated in Figure 6 in which the two force profiles are plotted for comparison. The implication of this similarity is that the surface morphology of P2VP−PEO is similar at these two solution pH's. A more rigorous comparison of the forces profiles at pH 9.3 and 6.6 in relation to surface morphology is made

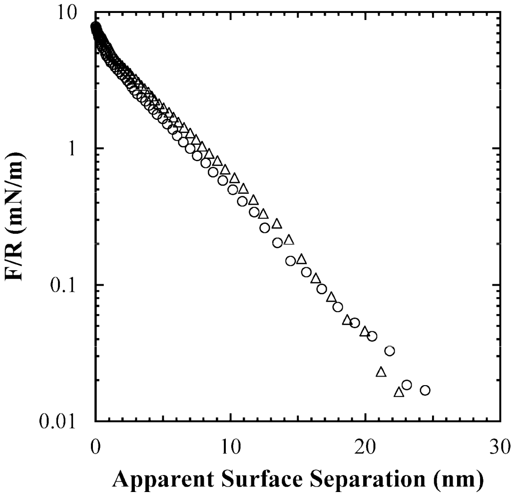

Figure 6. Comparison of the surface forces profiles for the interaction between two silica-adsorbed P2VP−PEO layers at (△) pH 9.3 and (○) pH 6.6. The polymer was initially adsorbed from a 10^{-3} M KNO_3 aqueous solution containing 500 ppm P2VP−PEO at pH 9.3 (same data as in Figure 5). Solution pH was subsequently decreased to pH 6.6 and surface forces measured after 12 h.

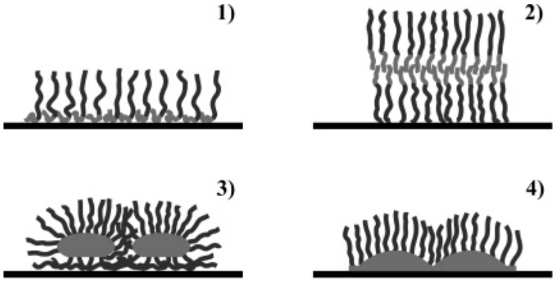

Figure 7. Schematic representations of the four possible surface morphologies that the silica-adsorbed P2VP−PEO micelles might adopt to ensure the P2VP blocks remain "shielded" from interaction with water. These morphologies are (1) a monolayer polymer brush anchored by the P2VP block, (2) a polymer bilayer where the inner leaflet attaches to silica via the PEO block and the outer leaflet exposes PEO to bulk solution, (3) surface micelles adsorbed via the PEO corona that have fused through interpenetration, and (4) fused surface hemimicelles that are adsorbed via the P2VP core.

below. But before this can be done it is necessary to discuss what surface morphologies might be expected when P2VP−PEO adsorbs to silica from a solution in which it exists as micelles.

Now, since P2VP−PEO exists as micelles in solution at pH 9.3, it is expected that it will adsorb as such and undergo whatever conformational change at the surface that is required to optimize its interaction with silica while maintaining optimal interaction with the aqueous environment. This conformational change, however, must be such that the P2VP block that forms the core of the micelle in bulk solution remains "shielded" from interaction with water, since the solution conditions are such that the hydrophobic driving force to self-assembly still remains. There are four possible surface morphologies that can achieve this, as illustrated in Figure 7: (1) a monolayer polymer brush in which P2VP is the anchor, (2) a polymer bilayer in which the inner leaflet attaches to silica via the PEO block while the outer leaflet exposes PEO to bulk solution, (3) surface micelles adsorbed via the PEO corona that have fused through interpenetration of the PEO chains, and (4) fused surface hemimicelles that are adsorbed via the P2VP core. We suggest interpenetrated micelles on the surface rather than discrete micelles since the surface excess of P2VP−PEO (Figure 2) is significantly higher than would be expected for such discrete adsorption. To highlight this point, we can make an upper estimate of the surface excess of P2VP−PEO adsorbed as discrete micelles if we assume hexagonal close packing on the surface. Using the polymer molecular weight and the polymer micelle's effective radius and aggregation number obtained from SANS measurements,[15] we estimate a surface excess of 1 mg m^2. This is less than one-third of that measured experimentally (Figure 2).

The form of the surface forces profiles does not allow us to categorically distinguish between each of these distinct surface morphologies since, in each case, it will be a PEO brush layer that is exposed to bulk solution, and so it is the interaction between PEO brush layers that is measured. We therefore interpret the force profiles using brush theory, below. It is interesting, however, to digress slightly at this point and speculate about which of the four surface morphologies is preferred by the P2VP−PEO system at high pH where solution conditions are conducive to self-assembly. It can be argued that the interaction of a P2VP−PEO micelle with the silica surface upon adsorption might facilitate the significant structural change required to form a polymer brush monolayer or bilayer. This would require the transfer of polymer chains from the micelle to the surface or else a cooperative rupture of the polymer micelle involving disentanglement of core polymer chains that are uncharged at pH 9.3. It is known however that polymer micelles in solution typically display slow kinetics: the transfer of individual copolymer chains between the micelle and bulk solution is so slow that they are considered to be kinetically frozen.[54] Additionally, the measured surface excess (Figure 2) is very high and so inconsistent with a polymer brush monolayer. Both points eliminate morphology 1 as a possibility. We have some preliminary data from the surface forces apparatus (not presented here) that give a hard-wall repulsion at 7 nm for the interaction between P2VP−PEO layers adsorbed on mica under the same solution conditions (i.e., pH 9.3). Typically in polymer brush systems, a hard-wall repulsion is obtained at surface separations of 1−2 nm.[41,55] A polymer brush bilayer (morphology 2) would give, at most, twice this hard-wall surface separation. An adsorbed layer comprised of interpenetrated micellar structures with the PEO corona attaching to the silica surface, or an interpenetrated hemimicelle layer anchored to silica via the P2VP core might, however, explain the relatively large surface separation for the hard-wall repulsion. Webber et al.[27] have found that when their polymeric micelle, lightly quarternized PDMA−PDEA, was adsorbed onto mica, it did so as a collapsed micelle. In this morphology the micelle remains intact but adopts a somewhat flattened layer structure rather than remaining as an undeformed sphere, the coronal chains of the micelle rapidly relaxing to the mica surface.[27] More work is currently underway in an attempt to elucidate the surface morphology of P2VP−PEO.

As discussed in detail above, we expect that, regardless of the detailed surface morphology of P2VP−PEO adsorbed onto silica from solution at pH 9.3, the surface interaction will be that of two PEO brushes (Figure 7). We have therefore fitted the force profile at pH 9.3 to the mean-field theory developed by Milner, Witten, and Cates (MWC)[56,57] that describes the interaction between two polymer brush layers as they are compressed. For comparison, we have done the same for the force profile at pH 6.6 since it appears similar in form to that at pH 9.3 (Figure 6). The MWC theory makes use of a parabolic segment density profile, thereby providing a more realistic representation of the polymer brush structure than the uniform segment density layer originally proposed by Alexander and de Gennes.[58,59] The expression used to calculate the theoretical force profiles was derived from the MWC theory by Kenworthy et al.[60] to express the distance dependence of the pressure, P, between brushlike layers, viz.

$$P(D) = P_0\left[\frac{L_0}{(D/2)^2} - \frac{D}{L_0^{\ 2}} + \frac{(D/2)^4}{L_0^{\ 5}}\right] \tag{1}$$

where

$$P_0 = \frac{kTN}{2}\left(\frac{\pi^2}{12}\right)^{1/3}\frac{a^{4/3}}{s^{10/3}} \tag{2}$$

L_0 is the equilibrium, noncompressed brush thickness, D the surface separation, T the temperature, k Boltzmann's constant, N the number of segments that comprise the brush block, and a the block segment length. For PEO, the segment length, a, is 0.35 nm.[60] The average distance, s, between the brush blocks is calculated using the expression $s = 2(\sigma/\pi)^{1/2}$,[61] where σ is the surface area per polymer chain. On the assumption that excluded volume is negligible, σ can be related to the polymer surface excess, Γ, obtained experimentally (see above), via the expression $\sigma = M/N_A\Gamma \times 10^{21}$, where M is the polymer molecular weight and N_A Avogadro's number.

Equation 1 can be integrated to give an estimate of the scaled repulsive force, $F(D)/R$, between a sphere of radius R and a flat surface as a function of surface separation, D, in the Derjaguin approximation,[62] since this is the geometry used in the AFM force measurements, viz.

$$\frac{F(D)}{R} = 2\pi E(D) = -2\pi \int P(D)\, \mathrm{d}D = 4\pi P_0\left[\frac{2L_0}{D} + \left(\frac{D}{2L_0}\right)^2 - \left(\frac{D}{2L_0}\right)^5 - \frac{9}{5}\right] \tag{3}$$

The s values used in fitting the pH 9.3 and 6.6 force profiles, i.e., 3.15 and 2.87 nm, respectively, were calculated from the surface excess data (Figure 2) using the relationships detailed above that relate surface excess, Γ, to s, the average distance between PEO blocks. As detailed above, in an AFM force experiment, zero surface separation is unknown so the surface separation plotted in the force profile is an intersurface distance that is offset by twice the thickness of the incompressible polymer layer. When fitting the force data to eq 3, this offset is accounted for by translating the force data along the x-axis by the offset distance, which can only be estimated. Typical offset values are 1−2 nm.[41,55] However here, since we believe P2VP−PEO adsorbs as a micelle, one might expect this offset value to be larger than typically used in such fittings. Indeed, an offset of 7 nm was selected here since it is the hard-wall separation obtained for the interaction between mica-adsorbed P2VP−PEO layers at pH 9.3 in surface forces apparatus measurements (unpublished data). L_0 is a fitting parameter selected on the basis of the range of the repulsive interaction. Hence, L_0 was adjusted within the ranges of 14−17 nm and 15.5−17.5 nm, for the offset pH 9.3 and 6.6 force data, respectively, in increments of 0.1−0.2 nm. The L_0 values that yield the best fit to the pH 9.3 and pH 6.6 force data are 15.8 and 16.0 nm, respectively. Note that these brush thicknesses compare favorably to the corona thickness of 14.9 nm that is obtained from small-angle neutron scattering measurements.[15] To scale the MWC fits to the experimental F/R values requires the use of a numerical prefactor.[55,61] In the present work, the prefactor used in fitting the pH 9.3 and pH 6.6 data was 7.5×10^{-2} and 4.0×10^{-2}, respectively.

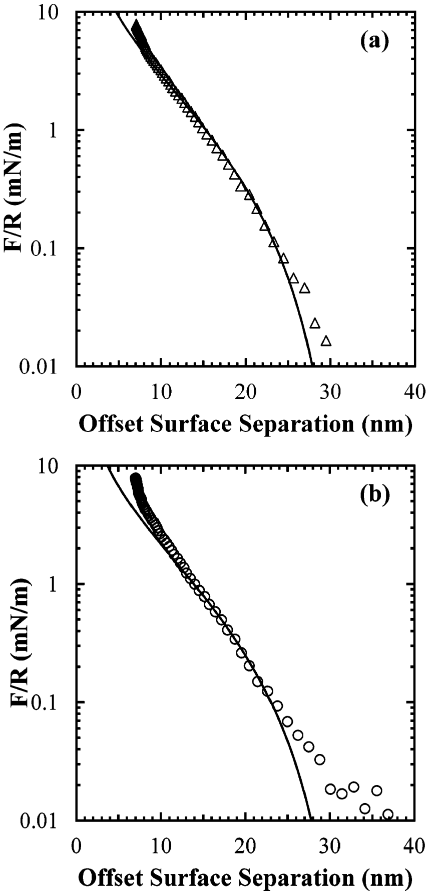

Figure 8. Offset surface forces profiles for the interaction between two silica-adsorbed P2VP−PEO layers at (a, △) pH 9.3 and (b, ○) pH 6.6. The data have been fitted to the Milner, Witten, and Cates (MWC) model for the compression of polymer brush layers. The solid lines are the MWC best fits. Note these are the same data presented in Figure 5 but offset by 7 nm to account for the thickness of an incompressible polymer layer on each surface.

Parts a and b of Figure 8 show the experimental force profiles for the silica-adsorbed P2VP−PEO interaction at pH 9.3 and 6.6, respectively, that have both been offset 7 nm to account for the compressed layer thickness, as discussed above. Also shown, as solid lines, are the MWC lines of best fit to these data. It is clear from Figure 8a that the MWC theory provides a good fit to the offset pH 9.3 force data. This is consistent with the suggested surface morphologies of P2VP−PEO at pH 9.3 discussed above.

In contrast, it is clear that the offset pH 6.6 force data cannot be fitted as well to the theory of MWC (Figure 8b). The fit is somewhat reasonable but not a truly good fit as obtained at pH 9.3. It should also be noted that there is no change in surface excess as a result of this decrease in solution pH (Figure 2); importantly, there is no measurable polymer desorption. The implication of these results is that there is surface morphological rearrangement as a result of the decrease in solution pH from 9.3 to 6.6. This is not unexpected and can be attributed to the significant charge density along the P2VP segment at pH 6.6 (the pK_a of the polymer is pH 5.9) which facilitates hydration of P2VP and segment−segment repulsion. There is now also the possibility of strong Coulombic interaction between the P2VP segments and the silica surface. The similarity in form and range of the repulsive interactions obtained at pH 9.3 and

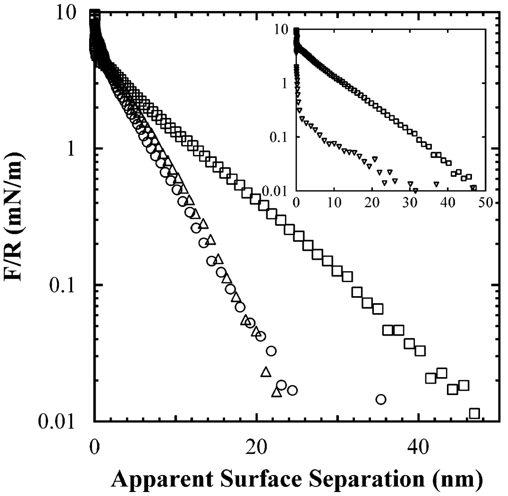

Figure 9. Surface forces profiles for the interaction between two silica-adsorbed P2VP−PEO layers adsorbed from a 10^{-3} M KNO_3 aqueous solution containing 500 ppm P2VP−PEO at pH 9.3. Surface forces were measured after 12 h equilibration at pH 9.3 (△) and then at 12 h intervals after subsequent pH adjustments to pH 6.6 (○) and then pH 3.6 (□). The inset compares the force profile at pH 3.6 (□) to the force profile for the interaction between two bare silica surfaces in a 10^{-3} M KNO_3 aqueous solution at pH 3.6 (▽).

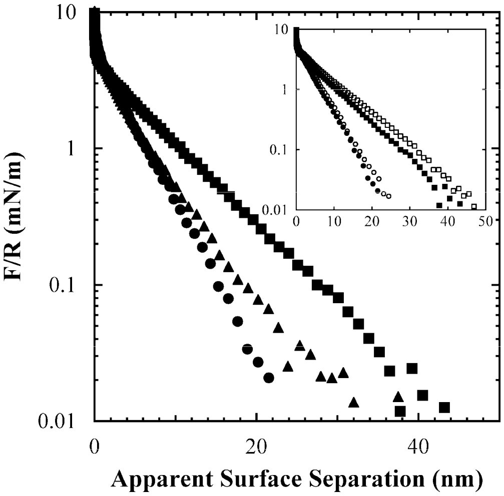

Figure 10. Surface forces profiles for the interaction between two silica-adsorbed P2VP−PEO layers adsorbed from a 10^{-3} M KNO_3 aqueous solution containing 500 ppm P2VP−PEO at pH 3.6. Surface forces were measured after 12 h equilibration at pH 3.6 (■) and then at 12 h intervals after subsequent pH adjustments to pH 6.6 (●) and then pH 9.3 (▲). In the inset, these profiles at pH 3.6 (■) and pH 6.6 (●) are compared to those obtained at the same pH's (pH 3.6 (□) and pH 6.6 (○)) when initial adsorption is at pH 9.3.

6.6 (Figure 6) indicates that the repulsion at pH 6.6 remains predominantly steric in origin with some brushlike character remaining.

A reduction in solution pH from 6.6 to 3.6 still results in a repulsive force profile (Figure 9). Recall that this pH change does not alter the surface excess (see above). The decay length is significantly altered and is now in agreement with that obtained for the interaction between bare silica surfaces under the same solution conditions (plotted together in the inset to Figure 9 for comparison). Indeed, the DLVO fit to these two sets of data yield Debye lengths of 8 ± 1 and 10 ± 1 nm for the interaction between P2VP−PEO layers, using a Hamaker constant of 10^{-20} J (see above),[50] and the interaction between bare silica surfaces, respectively. These both compare well with the theoretical Debye length of 9.6 nm for a 1:1 electrolyte at 10^{-3} M, implying that the repulsive force measured between the silica-adsorbed P2VP−PEO at pH 3.6 is indeed an electrical double-layer interaction. There is, however, a marked difference between both the range and magnitude of the repulsive interactions for these two force profiles. This can be explained in terms of surface charge densities. As noted above, the surface potential between two bare silica surfaces is −18 mV at pH 3.6 (Figure 4).[51] The DLVO fit to the P2VP−PEO data at pH 3.6 yields a surface potential of magnitude 90 mV. Hence, given that the P2VP blocks are positively charged at pH 3.6, the increase in the magnitude of the surface potential to 90 mV upon adsorption of the polymer can only be attributed to overcompensation of silica's surface charge by the polymer. That is to say, there is enough positively charged P2VP−PEO at the interface to reverse the sign of the net charge, resulting in a surface potential of +90 mV. This assertion is further supported by the high surface excess at this pH, i.e., 3.6 mg m^{-2} (see Figure 2).

It should be emphasized here that the interpretation of the surface forces data is solely in terms of polymer surface morphology. This argument is supported by the surface excess data presented in Figure 2 and discussed above, which show that after initial adsorption of P2VP−PEO at pH 9.3 subsequent pH changes do not result in any desorption or further adsorption of polymer. Thus, any changes in the surface forces profile from one solution pH to another can only reflect polymer conformational changes at the interface.

Effect of Adsorption History: Surface Interactions for Initial Adsorption at pH 3.6 Compared to Initial Adsorption at pH 9.3. Figure 10 contains the force profiles obtained from the pH low−high adsorption scheme, in which the silica surfaces were initially equilibrated in a pH 3.6 P2VP−PEO solution and pH subsequently increased to 6.6 and then 9.3. Note that the forms of the force profiles are similar to those obtained for the pH high−low adsorption scheme (Figure 9), but there is a clear difference in the trends of the profiles with pH: in the low−high scheme (Figure 10) the pH 6.6 and 9.3 force profiles no longer overlay each other, as in the high−low adsorption scheme. On first inspection, it also appears that the ranges of the interaction forces are different for the two adsorption schemes. However, plotting the force profiles for pH 3.6 and 6.6 for both adsorption schemes together (see the inset to Figure 10) shows that, at these two pH's, there is little difference between the force profiles at each pH. This highlights that, irrespective of adsorption scheme, the nature of the interaction forces, and therefore polymer surface morphology, is specific to solution pH. That is to say, polymer surface morphology is independent of the adsorption history. This is a particularly interesting result since it is well-established that many polymeric systems are nonergodic.[35−37] Indeed, the surface excess of the polymer at pH 6.6 is also independent of adsorption scheme, as seen when comparing Figures 2 and 3. There is some difference in surface excess for the two adsorption schemes at pH 3.6, but this has only a small impact on the force profile: the range of the profile is ∼49 nm at pH 3.6 in the high−low adsorption scheme and 44 nm in the low−high scheme. Nonetheless, both profiles at pH 3.6 can be fitted to DLVO theory, as discussed above, yielding a Debye length of 8 ± 1 nm irrespective of adsorption scheme, further emphasizing the similarity in form of the two force profiles and hence the similarity in surface morphology of the adsorbed polymer at this pH. The fitted surface potentials, +80 mV for the low−high adsorption scheme and +90 mV for the high−low adsorption scheme, reflect the difference in surface excess.

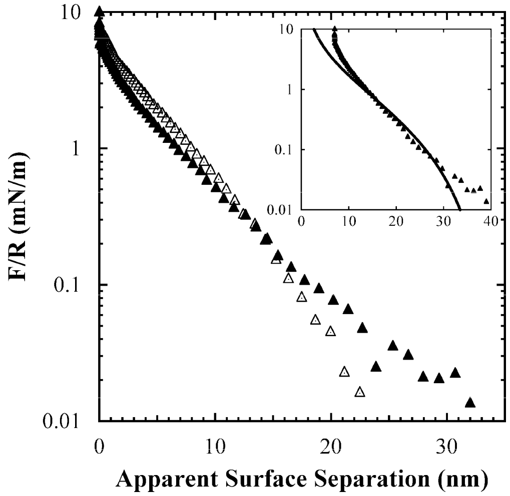

Figure 11. Surface forces profiles for the interaction between two silica-adsorbed P2VP–PEO layers adsorbed from a 10^{-3} M KNO_3 aqueous solution containing 500 ppm P2VP–PEO at pH 9.3: (▲) the polymer is initially adsorbed at pH 3.6 and the pH subsequently increased to 9.3; (△) the polymer is initially adsorbed at pH 9.3. The inset contains the force profile obtained at pH 9.3 after initial adsorption at pH 3.6 (▲) but offset by 7 nm to to account for the thickness of an incompressible polymer layer on each surface. An attempt was made to fit this forces profile to the Milner, Witten, and Cates (MWC) model for the compression of polymer brush layers. The solid curve is the line of best fit.

In contrast, the adsorption behavior of P2VP–PEO at pH 9.3 is nonergodic, being dependent on the adsorption history. This becomes apparent when the pH 9.3 force profiles obtained in the high–low and low–high adsorption schemes are plotted together in Figure 11. Clearly, the forms of the two force profiles are very different, as are the ranges of the interactions. In the high–low adsorption scheme the form of the pH 9.3 force profile is typical of a repulsive brush layer interaction. Indeed, the polymer brush theory of MWC[56,57] provides a good fit to the offset force data (as detailed above, Figure 8a) and as such implies that the polymeric micelles formed in solution at pH 9.3 remain intact upon adsorption at this solution pH (Figure 7). In contrast, when the polymer is initially adsorbed at low pH and solution pH subsequently increased to pH 9.3 in the low–high adsorption scheme, the surface interactions are not of the form of a polymer brush interaction. To highlight this, we have attempted to fit the force profile to MWC theory as done above. The offset force data at pH 9.3 and the corresponding MWC fit (solid line) are shown in the inset to Figure 11. It is clear that the force data cannot be fitted to the polymer brush theory of MWC. Indeed, the forms of the MWC theory curve and the experimental force profile are different. The implication therefore is that when P2VP–PEO is initially adsorbed at pH 3.6 and pH subsequently increased to pH 9.3, the polymer does not surface self-assemble to form a micellar structure, i.e., at pH 9.3 the surface morphology for silica-adsorbed P2VP–PEO is dependent on adsorption history.

The above discussion poses the question as to why at pH 9.3 the surface morphology of P2VP–PEO is history dependent. The answer lies in the influence that the silica surface has on self-assembly. Now, the evolution of the P2VP–PEO surface morphology brought about by changes in solution pH has been inferred from the surface forces, as described in detail above. This is summarized schematically for both adsorption schemes in Figure 12. At a solution pH of 9.3 P2VP–PEO self-assembles in solution and upon adsorption to silica at this pH maintains a micellar structure. The micellar surface structure only starts to break apart with a decrease in solution pH to 6.6 and further to 3.6. The polymer chains exist on the surface as unimers with each block able to optimize its interaction with the surface. At pH 3.6, below the polymer's pK_a of 5.9, the attachment to the surface is strongest by virtue of the electrostatic attraction between the high charge density P2VP block and the silica. In contrast, when the initial adsorption of P2VP–PEO is from a solution at pH 3.6, the polymer is a unimer in solution and adsorbs as such to the silica, adopting a similar conformation to that resulting from the adsorbed micelle breakup. An increase in pH to 6.6 simply reduces the electrostatic attraction between the P2VP block and the surface since at this pH the polymer has a low charge density. The surface morphology changes to reflect this. However, upon an increase in solution pH to 9.3, the surface self-assembly of preadsorbed P2VP–PEO unimers would require the cooperative detachment from the surface of a large number of polymer segments, almost to the extent of

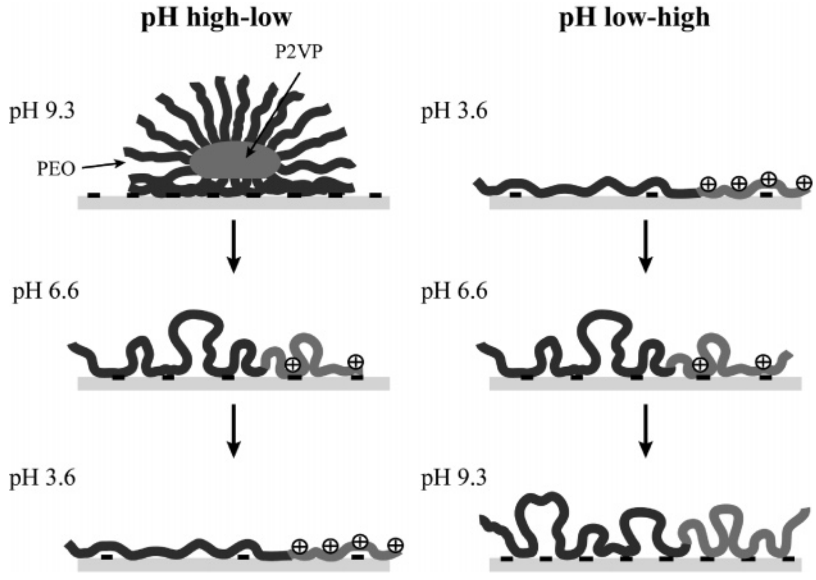

Figure 12. Schematic illustrating the evolution of the morphology of silica-adsorbed P2VP–PEO as a result of changes in solution pH. The series labeled "pH high–low" represents the evolution in surface morphology of the polymer with decreasing pH when initially adsorbed as a micelle from a pH 9.3 solution. The series labeled "pH low–high" represents the evolution in surface morphology of the polymer with increasing solution pH when initially adsorbed as a unimer from a pH 3.6 solution.

desorption. From a surface thermodynamics view point, the fluctuation in free energy required for such an event is insurmountable, and so no surface self-assembly is observed on the time scale of the experiment.

Conclusion

In this study we have investigated the history-dependent adsorption behavior of the pH-sensitive diblock copolymer P2VP−PEO as a function of solution pH using both ATR to measure the polymer surface excess and AFM to obtain, in situ, direct force measurements between the silica-adsorbed P2VP−PEO layers. The key observations taken from this study are the influence of solution conditions and adsorption history on the surface morphology of silica-adsorbed P2VP−PEO.

When the solution pH is 9.3, P2VP−PEO forms a micelle in solution and upon adsorption to silica at this pH remains self-assembled. However, when initial adsorption of the polymer is as a unimer, an increase in solution pH to 9.3 does not result in surface self-assembly since the cooperative detachment from the surface of a large number of polymer segments required to achieve this is energetically costly.

The adsorbed micelle can be broken up by a decrease in solution pH to below its pK_a with no polymer desorption. Presumably micelle breakup is due to the increased electrostatic segment−segment repulsion between the now ionized P2VP segments that form the micellar core at high pH's, while there is an increase in the affinity of the polymer for the negatively charged silica surface through attractive electrostatic interactions between silica and the ionized P2VP segments.

Interestingly, at solution pH's near and below its pK_a, P2VP−PEO exhibits ergodic behavior. The surface morphology appears uninfluenced by adsorption history, being the same at pH 3.6 and 6.6 whether the polymer is initially adsorbed as a unimer or as a micelle. A pH change from 3.6 to 6.6 or visa versa results in a subtle difference in surface morphology that can be explained in terms of changes in the electrostatic attraction between the P2VP block and the surface. This change in surface morphology between these two pH's appears reversible.

Acknowledgment. M.L.G. thanks the Australian Research Council for financial support of this project and the Particulate Fluids Processing Centre for infrastructure support. S.Mc.L. thanks the Australian government for an Australian Postgraduate Research Award.

References and Notes

(1) Gast, A. P. *Curr. Opin. Colloid Interface Sci.* **1997**, *2*, 258−263.
(2) Alexandridis, P. *Curr. Opin. Colloid Interface Sci.* **1996**, *1*, 490−501.
(3) Svensson, M.; Johansson, H.-O.; Tjerneld, F. *Amphiphilic Block Copolym.* **2000**, 377−407.
(4) Creutz, S.; Jerome, R.; Kaptijn, G. M. P.; van der Werf, A. W.; Akkerman, J. M. *J. Coat. Technol.* **1998**, *70*, 41−46.
(5) Savic, R.; Luo, L.; Eisenberg, A.; Maysinger, D. *Science (Washington, DC, U.S.)* **2003**, *300*, 615−618.
(6) Uhrich, K. E.; Cannizzaro, S. M.; Langer, R. S.; Shakesheff, K. M. *Chem. Rev.* **1999**, *99*, 3181−3198.
(7) Lavasanifar, A.; Samuel, J.; Kwon, G. S. *Adv. Drug Delivery Rev.* **2002**, *54*, 169−190.
(8) Gabizon, A. A. *Adv. Drug Delivery Rev.* **1995**, *16*, 285−294.
(9) Bae, Y.; Fukushima, S.; Harada, A.; Kataoka, K. *Angew. Chem., Int. Ed.* **2003**, *42*, 4640−4643.
(10) Lee, E. S.; Shin, H. J.; Na, K.; Bae, Y. H. *J. Controlled Release* **2003**, *90*, 363−374.
(11) Colfen, H. *Macromol. Rapid Commun.* **2001**, *22*, 219−252.
(12) Martin, T. J.; Prochazka, K.; Munk, P.; Webber, S. E. *Macromolecules* **1996**, *29*, 6071−6073.
(13) Gohy, J.-F.; Varshney, S. K.; Antoun, S.; Jerome, R. *Macromolecules* **2000**, *33*, 9298−9305.
(14) Gohy, J.-F.; Mores, S.; Varshney, S. K.; Zhang, J.-X.; Jerome, R. *e-Polym.* **2002**, *No. 21*.
(15) Nelson, A.; Schulz, J.; McLean, S. C.; Gee, M. L. Manuscript in preparation.
(16) Potemkin, I. I.; Kramarenko, E. Y.; Khokhlov, A. R.; Winkler, R. G.; Reineker, P.; Eibeck, P.; Spatz, J. P.; Moller, M. *Langmuir* **1999**, *15*, 7290−7298.
(17) Regenbrecht, M.; Akari, S.; Forster, S.; Mohwald, H. *J. Phys. Chem. B* **1999**, *103*, 6669−6675.
(18) Regenbrecht, M.; Akari, S.; Forster, S.; Mohwald, H. *Surf. Interface Anal.* **1999**, *27*, 418−421.
(19) Meiners, J. C.; Quintel-Ritzi, A.; Mlynek, J.; Elbs, H.; Krausch, G. *Macromolecules* **1997**, *30*, 4945−4951.
(20) Regenbrecht, M.; Akari, S.; Forster, S.; Netz, R. R.; Mohwald, H. *Nanotechnology* **1999**, *10*, 434−439.
(21) Connell, S. D.; Collins, S.; Fundin, J.; Yang, Z.; Hamley, I. W. *Langmuir* **2003**, *19*, 10449−10453.
(22) Hamley, I. W.; Connell, S. D.; Collins, S. *Macromolecules* **2004**, *37*, 5337−5351.
(23) Ma, N.; Zhang, H. Y.; Song, B.; Wang, Z. Q.; Zhang, X. *Chem. Mater.* **2005**, *17*, 5065−5069.
(24) Li, S. L.; Palmer, A. F. *Macromolecules* **2005**, *38*, 5686−5698.
(25) Rodriguez-Hernandez, J.; Babin, J.; Zappone, B.; Lecommandoux, S. *Biomacromolecules* **2005**, *6*, 2213−2220.
(26) Webber, G. B.; Wanless, E. J.; Armes, S. P.; Baines, F. L.; Biggs, S. *Langmuir* **2001**, *17*, 5551−5561.
(27) Webber, G. B.; Wanless, E. J.; Buetuen, V.; Armes, S. P.; Biggs, S. *Nano Lett.* **2002**, *2*, 1307−1313.
(28) Webber, G. B.; Wanless, E. J.; Armes, S. P.; Tang, Y. Q.; Li, Y. T.; Biggs, S. *Adv. Mater.* **2004**, *16*, 1794−+.
(29) Webber, G. B.; Wanless, E. J.; Armes, S. P.; Biggs, S. *Faraday Discuss.* **2005**, *128*, 193−209.
(30) Sakai, K.; Smith, E. G.; Webber, G. B.; Schatz, C.; Wanless, E. J.; Butun, V.; Armes, S. P.; Biggs, S. *Langmuir* **2006**, *22*, 5328−5333.
(31) Sakai, K.; Smith, E. G.; Webber, G. B.; Baker, M.; Wanless, E. J.; Butun, V.; Armes, S. P.; Biggs, S. *Langmuir* **2006**, *22*, 8435−8442.
(32) Sakai, K.; Smith, E. G.; Webber, G. B.; Wanless, E. J.; Butun, V.; Armes, S. P.; Biggs, S. *J. Colloid Interface Sci.* **2006**, *303*, 372−379.
(33) Leckband, D.; Sheth, S.; Halperin, A. *J. Biomater. Sci., Polym. Ed.* **1999**, *10*, 1125−1147.
(34) Halperin, A. *Langmuir* **1999**, *15*, 2525−2533.
(35) Dahlgren, M. A. G.; Hollenberg, H. C. M.; Claesson, P. M. *Langmuir* **1995**, *11*, 4480−4485.
(36) Claesson, P. M.; Dahlgren, M. A. G.; Eriksson, L. *Colloids Surf., A* **1994**, *93*, 293−303.
(37) Maurdev, G.; Meagher, L.; Ennis, J.; Gee, M. L. *Macromolecules* **2001**, *34*, 4151−4158.
(38) Barder, T. J.; Dubois, P. D. United States Patent No. 4,983,369, Jan 1991.
(39) Ducker, W. A.; Senden, T. J.; Pashley, R. M. *Langmuir* **1992**, *8*, 1831−1836.
(40) Cleveland, J. P.; Manne, S.; Bocek, D.; Hansma, P. K. *Rev. Sci. Instrum.* **1993**, *64*, 403−405.
(41) McLean, S. C.; Lioe, H.; Meagher, L.; Craig, V. S. J.; Gee, M. L. *Langmuir* **2005**, *21*, 2199−2208.
(42) Harrick, N. J. *Internal Reflection Spectroscopy*; Interscience Publishers: New York, 1967.
(43) Neivandt, D. J.; Gee, M. L. *Langmuir* **1995**, *11*, 1291−1296.
(44) Trau, M.; Grieser, F.; Healy, T. W.; White, L. R. *Langmuir* **1992**, *8*, 2349−2353.
(45) Vig, J. R. *J. Vac. Sci. Technol. A* **1983**, *3*, 1027−1034.
(46) Kern, W. *J. Electrochem. Soc.* **1990**, *137*, 1887−1892.
(47) Mubarekyan, E.; Santore, M. M. *Macromolecules* **2001**, *34*, 7504−7513.
(48) Hartley, P. G. In *Colloid-Polymer Interactions: From Fundamentals to Practice*; Farinato, R. S., Dubin, P. L., Eds.; John Wiley & Sons: New York, 1999.
(49) McCormack, D.; Carnie, S. L.; Chan, D. Y. C. *J. Colloid Interface Sci.* **1995**, *169*, 177−196.
(50) Hough, D. B.; White, L. R. *Adv. Colloid Interface Sci.* **1980**, *14*, 3−41.
(51) Hartley, P. G.; Larson, I.; Scales, P. J. *Langmuir* **1997**, *13*, 2207−2214.
(52) Ruths, M.; Sukhishvili, S. A.; Granick, S. *J. Phys. Chem. B* **2001**, *105*, 6202−6210.
(53) Fleer, G. J.; Cohen Stuart, M. A.; Scheutjens, J. M. H. M.; Cosgrove, T.; Vincent, B. *Polymers at Interfaces*; Chapman & Hall: London, 1993.
(54) Zhang, L.; Shen, H.; Eisenberg, A. *Macromolecules* **1997**, *30*, 1001−1011.

(55) Pasche, S.; Textor, M.; Meagher, L.; Spencer, N. D.; Griesser, H. J. *Langmuir* **2005**, *21*, 6508−6520.
(56) Milner, S. T. *Europhys. Lett.* **1988**, *7*, 695−699.
(57) Milner, S. T.; Witten, T. A.; Cates, M. E. *Macromolecules* **1988**, *21*, 2610−2619.
(58) Alexander, S. *J. Phys. (Paris*) **1977**, *38*, 983−987.
(59) de Gennes, P. G. *Adv. Colloid Interface Sci.* **1987**, *27*, 189−209.
(60) Kenworthy, A. K.; Hristova, K.; Needham, D.; McIntosh, T. J. *Biophys. J.* **1995**, *68*, 1921−1936.
(61) Efremova, N. V.; Bondurant, B.; O'Brien, D. F.; Leckband, D. E. *Biochemistry* **2000**, *39*, 3441−3451.
(62) Derjaguin, B. V. *Kolloid Z.* **1934**, *69*, 155−164.

MA0706780